UPSTREAM GENERATION OF SOLITONS: NUMERICAL ANALYSIS OF THE DEPENDENCE ON KEY PARAMETERS

B. E Protopopov

UDC 532.59

Lately researchers have been increasingly interested in a recently discovered phenomenon: the ability of a source of disturbance that is moving along the surface of a fluid to generate an outgoing soliton-like wave that moves ahead of the source in the same direction as the source [1-6]. Analysis of soliton generation is quite a difficult problem, since it requires the use of fairly complex mathematical models which take into account both the nonlinearity and the dispersion of waves (it is the peculiar balance of these effects that constitute the mechanism of the phenomenon). Therefore numerical methods predominate among the methods used to study this process.

Another factor complicating the problem is the large number of governing parameters: in addition to the horizontal coordinate x (the motion is assumed to be plane-parallel and to depend on depth only on the average) and time t, there is the acceleration of gravity g, the density ρ, and depth h = const of the fluid, as well as those parameters characterizing the source of the disturbance. As the latter, we consider the region of surface pressure p(x, t), which is conveniently written in the form [1-6]

$$p(x, t) = p_0(\xi) = \begin{cases} p_m \cos^2(\pi\xi/2), & |\xi| \leqslant 1, \\ 0, & |\xi| > 1 \end{cases}$$

($\xi = (x - ct)/\ell$ is the local coordinate in a moving frame of reference that is tied to the source of disturbance). Thus, the region of pressure is characterized by its rate of motion c = const, its maximum deviation from zero $p_m = p_0(0)$ (equal to max $p_0(\xi)$ for $p_m > 0$), and its effective length $\ell = f/p_m$, where f is the total pressure on the surface of the fluid (henceforth used as the governing parameter in place of p_m):

$$f = \int_{-\infty}^{\infty} p(x, t)\, dx = l \int_{-1}^{1} p_0(\xi)\, d\xi.$$

Transforming to dimensionless variables by scaling all quantities by the term $\rho^\beta g^\gamma h^\delta$ with the appropriate exponents β, γ, and δ and keeping the previous notation, we obtain $\rho = g = h = 1$ in the new variables; all unknowns will be functions of c, ℓ, and f (in addition to depending on x and t).

Due to the three-dimensionality of the governing parameter space, numerical analysis of the process of soliton generation is very laborious, and at present is far from complete. The available information on the question of the dependence of this process on external conditions [1-6] can be significantly augmented: the present paper is devoted to this goal.

1. Mathematical Formulation and Computational Algorithm. The process of soliton generation was modeled within the framework of the generalized Boussinesq approximation [1, 3]. The unknown functions are the free surface elevation $\eta(x, t)$ and the horizontal component of the velocity averaged over depth u(x, t). Their evolution is obtained from the equations

$$\eta_t + [(1 + \eta)u]_x = 0, \quad u_t + uu_x + \eta_x + p_x = (1/3)u_{txx} \tag{1.1}$$

(the letter subscript denotes partial differentiation with respect to the corresponding variable), with initial conditions

$$\eta = \eta_0(x), \quad u = u_0(x) \text{ at } t = 0. \tag{1.2}$$

Novosibirsk. Translated from Prikladnaya Mekhanika i Tekhnicheskaya Fizika, No. 1, pp. 88-94, January-February, 1993. Original article submitted April 4, 1991; revision submitted January 16, 1992.

0021-8944/93/3401-0085$12.50

The model is obtained with the following assumptions concerning the characteristic values of the amplitude α and the length λ of the wave being studied [1, 3]:

$$\alpha \ll 1,\ \lambda \gg 1,\ \alpha\lambda^2 = O(1). \tag{1.3}$$

For ease of construction of the difference scheme, the system of equations (1.1), (1.2) is conveniently rewritten in the form

$$\eta_t + q_x = 0,\ w_t + s_x = 0; \tag{1.4}$$

$$\eta = \eta_0(x),\ w = w_0(x) \quad \text{at} \quad t = 0, \tag{1.5}$$

where

$$q(x,\ t) = (1 + \eta)u; \tag{1.6}$$

$$w(x,\ t) = u - (1/3)u_{xx}; \tag{1.7}$$

$$s(x,\ t) = (1/2)u^2 + \eta + p, \tag{1.8}$$

and the initial function $w_0(x)$ is determined in terms of $u_0(x)$ in accordance with (1.7). Initially the fluid is at rest, i.e.,

$$\eta_0(x) \equiv -p(x,\ 0),\ w_0(x) \equiv 0\ (\Leftarrow u_0(x) \equiv 0).$$

To carry out the calculations, it is necessary to limit the range of x ($-\ell_1 \leq x \leq \ell_2$) with the statement of appropriate boundary conditions. In this case, the lateral boundaries are considered to be impermeable:

$$u = 0 \quad \text{for } x = -l_1,\ x = l_2; \tag{1.9}$$

$$q = 0 \quad \text{for } x = -l_1,\ x = l_2. \tag{1.10}$$

Conditions (1.9), (1.10) can be treated as the preservation of the initial, quiescent state of the fluid far from the source of disturbance, which holds in view of the finite wave propagation velocity. This is valid only up to the moment of time determined by the selected values of ℓ_1 and ℓ_2 (here $\ell_1 = 2$, $\ell_2 = 178$).

The numerical algorithm for solving problem (1.4)-(1.10) was constructed using finite differences. Discretization in time was done using the implicit Crank–Nicholson scheme

$$\eta^{n+1,k+1} + \frac{\Delta t}{2} q_x^{n+1,k} = \eta^n - \frac{\Delta t}{2} q_x^n,\ w^{n+1,k+1} + \frac{\Delta t}{2} s_x^{n+1,k} = w^n - \frac{\Delta t}{2} s_x^n$$

(Δt is the time step; the first superscript is the time step number, the second is the iteration number). An iterative process is needed at each time step because the scheme is implicit and because of the nonlinearity of (1.6) and (1.8).

Spatial discretization of the variables is done on a mesh with spaced nodes, viz; mesh functions $\eta_{i-1/2}$, $s_{i-1/2}$, $p_{i-1/2}$ ($i = 1, \ldots, M$), w_i ($i = 1, \ldots, M-1$), q_i, u_i ($i = 0, \ldots, M$) are used. Here, f_ν denotes $f(x_\nu)$ ($x_\nu = -\ell_1 + \nu\Delta x$, $\Delta x = (\ell_1 + \ell_2)/M$ is the step in x, and M is an integer). With such a distribution of mesh nodes, the only possible approximation of the first derivatives in terms of x are symmetric differences. The values of the functions themselves between nodes are of necessity determined by finite differences. For example

$$(q_x)_{i-1/2} \approx (q_i - q_{i-1})/\Delta x,\ u_{i-1/2} \approx (u_i + u_{i-1})/2.$$

The boundary conditions are satisfied exactly: at the ends of the interval $[-\ell_1, \ell_2]$, only the nodal functions q and u are distributed, their boundary values being prescribed according to (1.9) and (1.10).

Problem (1.7), (1.9) for establishing the velocity u in terms of the known function w is sufficiently simple that its finite difference implementation using the usual three-point approximation of the second derivatives does not cause difficulty. The difference scheme constructed is of second order accuracy in both independent variables; it is conservative due to the equation approximating the divergence, and being implicit, it has a large margin of stability.

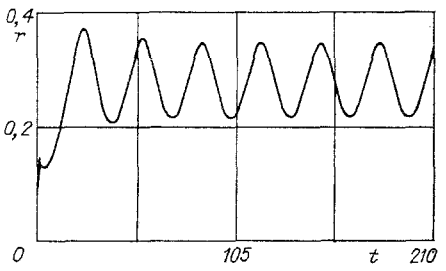

Fig. 1

Calculations were done on a mesh with parameters $\Delta x = 0.2$ and $\Delta t = 0.1$, which ensures reasonably high accuracy of the numerical solution to the problem. A further decrease by a factor of two of the mesh parameters resulted in no more than a 3% change in the wave drag r(t) in the norm which is the discrete analog to the norm of the space of continuous functions (the results of varying the mesh step size for fixed choice of parameters c, ℓ, and f can be found in [5, 6]).

2. Computations; Results. Without touching on the question of the behavior of the function $\eta(x, t)$ (the general wave pattern behaves as in [2-4]), we limit our examination to an important integral characteristic of the process: the wave drag r(t), defined by [1]:

$$r(t) = \int_{-l_1}^{l_2} p(x, t) \frac{\partial}{\partial x} \eta(x, t)\, dx = \int_{-1}^{1} p_0(\xi) \frac{\partial}{\partial \xi} \tilde{\eta}(\xi, t)\, d\xi, \quad \tilde{\eta}(\xi, t) = \eta(\xi l + ct, t).$$

The function r(t), doubtless of interest in itself as the horizontal component of the reaction force of the fluid to an exterior action, also carries in addition general information on the process of soliton generation. In particular, r(t) oscillates with the period of soliton generation, while by its amplitude one can judge the amplitude of the solitons being formed (the results of [1-6] indicate the approximate proportionality of these amplitudes). Below we will use only the orthonormal quantity $r'(t) = r(t)/f$ while keeping the original notation (without the prime).

The function r(t) has the characteristic form shown in Fig. 1 (computed for $c = \ell = 1$, $f = 0.2$), and can be represented by

$$r(t) = \langle r \rangle + v(t - \Delta T) + r_0(t), \quad \langle r \rangle = \lim_{t \to \infty} \frac{1}{t} \int_0^t r(\tau)\, d\tau,$$

where $\langle r \rangle$ is the mean value of r(t); v(t) is a function that oscillates about zero with period T and amplitude a: $v(t + T) = v(t)$; $a = v_{max} - v_{min}$; $v_{max} = \max v(t)$; $v_{min} = \min v(t)$. The phase shift Δt is determined from the condition $v(0) = v_{max}$, $0 \le \Delta T < T$. The function $r_0(t)$ is introduced to describe the behavior of r(t) at early times: $r_0(t) \to 0$ for $t \to \infty$.

Thus, for large t, r(t) is reasonably completely characterized by the following parameters: the mean $\langle r \rangle$ and maximum $r_{max} = \langle r \rangle + v_{max}$ values of the wave drag, the frequency $\omega = 2\pi/T$, and the amplitude a of the oscillations of v(t), and the relative phase shift $\Delta T/T$.

Some computational results for the most significant of the enumerated quantities are given below as functions of c, ℓ, and f. The following methods of parameter variation were considered:

1) $c = F$, $\ell = 1$, $f = 0.2$;

2) $c = F$, $\ell = F^2$, $f = 0.2\ F^4$;

3) $c = 1$, $\ell = F^{-2}$, $f = 0.2$;

4) $c = F$, $\ell = 1$, $f = 0.15$.

Methods 1 and 3 evidently vary the velocity and the length of pressure region, respectively; 2 varies the dimensional depth of the fluid $h \sim F^{-2}$ while the other dimensional quantities

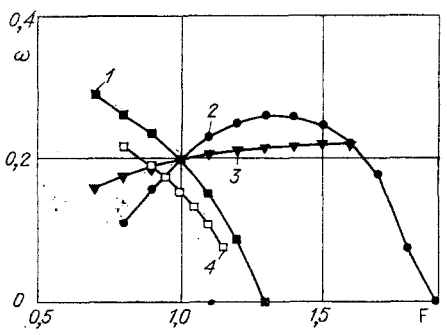

Fig. 2

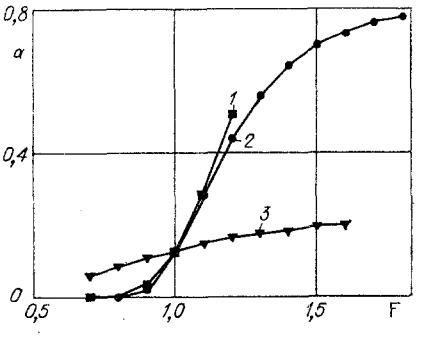

Fig. 3

are held constant (because h is used in scaling, this leads to the indicated dependence of c, ℓ, and f on F). Method 4 is analogous to the first method; the computational results for this method are taken from [4] and introduced here for comparison. The parameter F in method 3 has the sense of the Froude number in terms of the length of the pressure region ($F = F_\ell = c/\sqrt{\ell}$), while in the other methods it is the Froude number in terms of the depth, equal to the dimensionless velocity ($F = F_h = c$).

The methods chosen for varying the governing parameters for any unknown $b = b(c, \ell, f)$ are placed in the corresponding function $b_i(F)$ ($i = 1, 2, 3, 4$), where $b_1(F) = b(F; 1; 0.2)$, $b_2(F) = F^{-2\delta}b(F; F^2; 0.2\,F^4)$, $b_3(F) = b(1; F^{-2}; 0.2)$, $b_4(F) = b(F; 1; 0.15)$. The presence of the normalizing factor $F^{-2\delta} = \ell^{-\delta}$ (δ is the exponent from the scaling multiplier $\rho^\beta g^\gamma h^\delta$ for the quantity b) in the second relation reflects the fact that in this case, the depth of the fluid is considered to be variable, and the scale of all parameters naturally is tied not to h, but to the dimensional length of the pressure region, which is considered to be unchanging. In Figs. 2-5, points 1-4 (joined by lines of clarity) correspond in number order to the functions $b_i(F)$, where b is understood to mean any parameter characterizing the wave drag.

Figure 2 shows the oscillation frequency ω of the function v(t) or the frequency of soliton generation. The behavior of $\omega_i(F)$ is qualitatively different for different F_h due to the velocity and the depth ($i = 1$ and 2). In the first case, the frequency is monotonic and dies off quite rapidly; in the second it grows to its maximum of $\omega_{max} = 0.263$ at $F = 1.34$, after which it also rapidly drops to zero. Variation of the length of the interval over which the surface pressure is distributed leads to relatively less though still noticeable change in the frequency (line 3). Evidently the critical value is not the pressure distribution but the total force, which was constant: $f = 0.2$. For comparison, results from [4] are given, which varies the governing parameter using method 4 (analogous to method 1) but with a smaller value of f. Accordingly, line 4 virtually duplicates 1 at a lower level.

Figure 2 makes it possible to estimate the upper boundary of the interval for the value of F_h at which soliton generation occurs. With increasing F_h, soliton formation comes to a halt because of the unbounded growth in the generation period, i.e., the decrease of the frequency to zero. Clearly the upper critical value of the Froude number F_+ is in the interval [1.2; 1.3] for method 1 and in [1.8; 1.9] for method 2. The first of these intervals is in good agreement with the results of [2, 4], however, variation in fluid depth was not considered in these works. Nevertheless, the approximate relation constructed in [2]

$$F_+ = 1 + p_m/(0{,}7 + p_m) \tag{2.1}$$

can also be used to estimate F_+ with variation in depth if in neglecting the weak dependence of ω on ℓ, the choice of parameters $c = F$, $\ell = F^2$, $f = 0.2F^4$ is considered equivalent to the choice $c = F$, $\ell = 1$, $f = 0.2\,F^4$. Then $p_m = f$ and the critical Froude number is determined from

$$F_+ = 1 + 0{,}2F_+^4/(0{,}7 + 0{,}2F_+^4),$$

which gives $F_+ \approx 1.71$. That this value is somewhat at odds with the condition $F_+ \in [1.8; 1.9]$ is probably caused by inadequate accuracy in (2.1), which generally speaking was constructed for calculational approximations within the limits $1.0 \leq F_+ \leq 1.4$ [2].

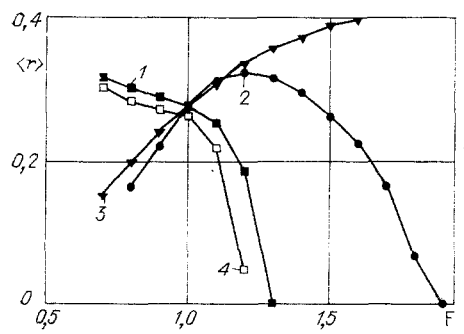

Fig. 4

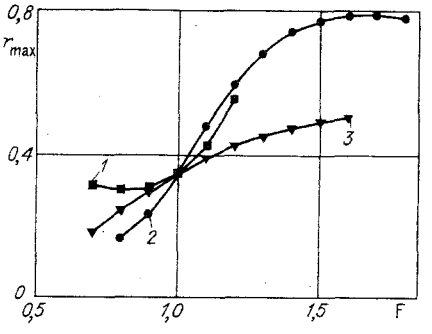

Fig. 5

The oscillation amplitude a of the wave drag is shown in Fig. 3. Here the difference between the two methods for varying F_h (by velocity or depth) is insignificant and according to Fig. 2, mainly consists of the fact that curve 2 extends to higher values of F for which $a_2(F)$ approaches a constant value as F_+ is approached. With decreasing F, curves 1 and 2 rapidly fall to zero, thereby determining the lower boundary F_- of the interval for F_h for the phenomenon as being in the interval [0.7; 0.8].

It was noted in [4] that for $F_h < 0.8$, the oscillation amplitude of the wave drag is very small compared to ⟨r⟩, which is in good agreement with the results given here. However, significantly lower value for F_- ($F_- = 0.2$) was given as the lower boundary. The difference can be explained by the fact that the value given was obtained by measuring the amplitude of r(t) at small t. Due to marked damping of the oscillations in r(t), observed for $F_h < 1$ and also noted in [4], this measured value significantly exceeds the amplitude of r(t) at large t, i.e., the value of a [function v(t) is the purely periodic part of the wave drag, which damps the part contained in $r_0(t)$].

Figure 4, which shows the mean value ⟨r⟩ of the wave drag quantitatively reduces to Fig. 2. Here the maximum $\langle r\rangle_2(F)$ is 0.324 at F = 1.21. Curve 4 is constructed according to the results from [4], which uses method 4 for varying the governing parameters. As before, there is good qualitative agreement between curves 1 and 4 with a small quantitative discrepancy caused by the difference in the values of f.

Figure 5 shows the maximum value r_{max} for the wave drag. This also can be considered as analogous to Fig. 3. However, note that in the case of variation of fluid depth, $r_{max}(F)$ has a maximum of 0.791 at the point F = 1.66.

3. Conclusions. These computational results augment significantly existing data on the question of the dependence of wave drag (and soliton generation as a whole) on external conditions. In particular the variation of fluid depth, which is undoubtedly of interest, has been examined here. The existence of different critical values for the depth h_1, h_2, and h_3 at which the corresponding frequencies of soliton generation and the mean and maximum values (in time) of the wave drag are maximal has been established. Thus, for a pressure region with parameters c, ℓ, and f related by $c = \sqrt{\ell}$, $f = 0.2\ \ell^2$, we have $h_1 = 0.557\ \ell$ ($\max\omega(F) = 0.263/\sqrt{\ell}$), $h_2 = 0.684\ \ell$ ($\max\langle r\rangle(F) = 0.324$), $h_3 = 0.363\ \ell$ ($\max r_{max}(F) = 0.791$).

It is known that soliton generation is observed only in a fairly narrow interval of Froude numbers which contains unity. With decreasing F_h, the process no longer occurs, because the amplitude of the solitons being formed tends to zero. On the other hand the process comes to a stop for increasing F_h because of unbounded growth in the period of generation. In this case, as shown by the calculations, the upper boundary of the interval of admissible F_h depends on other similarity numbers (ℓ and f) and can exceed significantly the limiting value of the propagation velocity of nonlinear steady waves. This can be interpreted as favoring the existence of an unsteady process, or as evidence of the inadequacy of the model or more precisely, of its improper application at certain points (c, ℓ, f) in the governing parameter space.

Indeed, condition (1.3), which is sufficient for the validity of the Boussinesq approximation, was not always satisfied in the calculations. Thus $\alpha > 1$ for $F > 1.13$ in the case of variation of c and also for $F > 1.08$ when h is varied. The applicability of the model when condition (1.3) is not met can be judged by comparison with experiment [4] and with

calculations using a more general model of potential flow of an ideal fluid [5, 6]. In doing this, some discrepancy of quantitative results was also observed, which grows with increasing power of the source of disturbance. However, this does not cause any qualitative disparity in the results (the value of α in this case reaches 0.7). Note also that within the limits of another approximate model (the Green–Hardy model), soliton generation is computed right up to $F_h = 1.4$ [2]; no reason being noted for cessation of generation for $F_h > 1.4$.

Thus, it would seem that the possibility of generating solitons with amplitudes and velocities markedly exceeding the limiting values of these parameters for steady waves is explained not so much by the weak nonlinearity of the model being used as by the nature of the phenomenon, to wit, the presence of a forcing term which significantly reduces the degrees of freedom of the resultant solitons. However, one can probably expect some reduction in the upper boundary of attainable values for F_h for the more general models, due to the loss of stability of large-amplitude waves (the development of wave instability with increasing power of the source of disturbance has been noted in experiments [4] and was observed by the author while doing numerical calculations of the problem that uses a potential model [5, 6]).

LITERATURE CITED

1. D. M. Wu and T. Y. Wu, "Three-dimensional nonlinear long waves due to moving surface pressure," in Proceedings of the 14th Symposium on Naval Hydrodynamics, Michigan (1982).
2. R. C. Ertekin, W. C. Webster, and J. V. Wehausen, "Waves caused by a moving disturbance in a shallow channel of finite width," J. Fluid Mech., 169, 275 (1986).
3. T. Y. Wu, "Generation of upstream advancing solitons by moving disturbances," J. Fluid Mech., 184, 75 (1987).
4. S. J. Lee, G. T. Yates, and T. Y. Wu, "Experiments and analyses of upstream-advancing solitary waves generated by moving disturbances," J. Fluid Mech., 199, 563 (1989).
5. B. E. Protopopov, "Numerical investigation of soliton generation by a moving region of surface pressure," Int. Series Num. Math., 99, 347 (1991).
6. B. E. Protopopov, "Numerical modeling of soliton generation by a moving region of surface pressure," Prikl. Mekh. Tekh. Fiz., No. 3 (1991).

INFLUENCE OF THE OUTER FEEDBACK LOOP PARAMETERS ON THE FREE OSCILLATIONS OF THE FLOW OF AN UNDEREXPANDED JET PAST A FINITE OBSTACLE

S. G. Mironov

UDC 534.2:532

The oscillation interaction of supersonic gas jets with obstacles was studied at the end of the 1920s [1] and has found broad application. However, the problem of the mechanism supporting the oscillations remains obscure. Virtually all hypotheses which purport to explain this phenomenon are based on channels of direct and feedback coupling of the freely oscillating jet–obstacle system. These hypotheses can be divided into two basic groups: feedback is accomplished by waves in the shock layer between the obstacle and the central shock wave [2-4]; or feedback is accomplished by sound waves which propagate in the medium surrounding the jet [5]. These models with equal plausibility describe the motion of the flow elements as observed in shadowgraphs, and they determine the pulsation frequency with reasonable accuracy. However, they do not permit determination of the region in which oscillations take place; nor do they explain the jump in frequencies. An attempt was made in [6] to work with both models and to find their regions of applicability. On the basis of a schlieren analysis of the interaction of a weakly underexpanded jet with an obstacle, it was shown that outer feedback dominates when the obstacle diameter d_o exceeds the diameter of the exit nozzle cross section d_a by a factor of four or more ($d_o/d_a > 4$); on the other hand, inner feedback dominates when $d_o/d_a < 2$: the physical meaning of this criterion has

Novosibirsk. Translated from Prikladnaya Mekhanika i Tekhnicheskaya Fizika, No. 1, pp. 94-100, January-February, 1993. Original article submitted December 27, 1991.

 0021-8944/93/3401-0090$12.50